JCTC Journal of Chemical Theory and Computation

Article

pubs.acs.org/JCTC

Thermal Gradients on Graphene to Drive Nanoflake Motion

Matthew Becton and Xianqiao Wang*

College of Engineering, University of Georgia, Athens, Georgia 30602, United States

ABSTRACT: Thermophoresis has been emerging as a novel technique for manipulating nanoscale particles. Materials with good thermal conductivity and low surface friction, such as graphene, are best suited to serve as a platform for solid−solid transportations or manipulations. Here we employ nonequilibrium molecular dynamics simulations to explore the feasibility of utilizing a thermal gradient on a large graphene substrate to control the motion of a small graphene nanoflake on it. Attempts to systematically investigate the mechanism of graphene−graphene transportation have centered on the fundamental driving mechanism of the motion and the quantitative effect of significant parameters such as temperature gradient and geometry of graphene on the motion of the nanoflake. Simulation results have demonstrated that temperature gradient plays the pivotal role in the evolution of the motion of the nanoflake on the graphene surface. Also, the geometry of nanoflakes has presented an intriguing signature on the motion of the nanoflake, which shows the nanoflakes with a circular shape move slower but rotate faster than other shapes with the identical area. It reveals that edge effects can stabilize the angular motion of thermophoretically driven particles. An interesting relation between the effective initial driving force and temperature gradient has been quantitatively captured by employing the steered molecular dynamics. These findings will provide fundamental insights into the motion of nanodevices on a solid surface due to thermophoresis, and will offer the novel view for manipulating nanoscale particles on a solid surface in techniques such as cell separation, water purification, and chemical extraction.

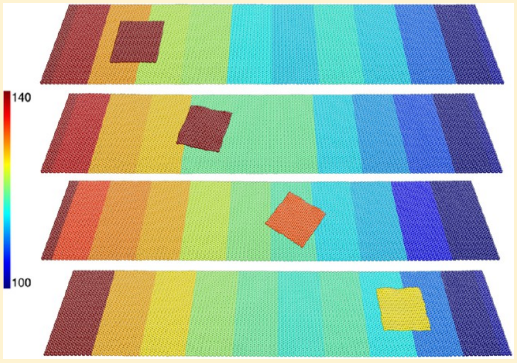

1. INTRODUCTION

Recent years have witnessed the explosive growth of interest in nanoscale manipulations and transportations. As nanoscience rapidly develops, experimental techniques for the manipulation of material at the nanoscale have gained unparalleled accuracy, as reflected in the development and utilization of atomic force microscopy,[1−3] magnetic and optical tweezers,[4−7] and nanoindentation,[8,9] to name a few here. There are many routes for this manipulation: mechanical,[10] electrostatic,[11] ultrasonic[12] and surface dynamic[13] interactions, to name a few. An old material manipulation technique that is gaining new influence in the nano fields is that of thermophoresis, the motion of objects away from a heat source.[14−16] Thermophoresis is a very interesting phenomenon at the nanoscale, with the effective driving "force" rather ambiguous[17] but most likely arising from nonsymmetric phonon effects between the hot and cool edges of the chosen vehicle.[18] An induced thermal gradient can provide more sensitivity in manipulating structures than mechanically inclined methods such as atomic force microscopy, optic tweezers, nano pipet, etc.

Carbon based nanomaterials, such as carbon nanotubes and graphene sheets, which have a homogeneous sp^2 hexagonal crystalline structure, thus fit both of these criteria excellently due to their exceptional physical properties. Carbon−carbon sliding, especially in the form of carbon nanotube bearings, has been studied extensively.[19−23] In addition, there has been both simulation and experimental work pertaining to thermophoretic motion in double-walled carbon nanotubes and nanoparticles confined in carbon nanotubes,[17,24−30] but very little work on thermophoresis has been performed with planar graphene.[31,32] To the best knowledge of the authors, there has been no research investigating the thermophoretic motion of graphene nanoflakes across graphene. Thermophoretic graphene−graphene sliding has multiple applications, from the precise positioning of large sections of graphene to rapid, controlled motion of nanoparticles of various geometries to driving a structural change with waste heat for better governance of thermal exhaust. To better use this many-faceted and multipurpose technique to its full capacity, persistent efforts to unravel the fundamental mechanism of graphene−graphene sliding from the perspective of atomic level are worthwhile to make, with both computational and experimental investigations.

This work seeks to employ nonequilibrium molecular dynamics simulation to determine the effect of varying distinct parameters (geometry, temperature gradient, nanoflake area) on the thermophoretic motion of graphene nanoflakes across a graphene substrate. Section2 describes the details of the simulation methodologies. Section3 presents and analyzes the results obtained by varying the initial parameters of thermal gradient magnitude, geometry of the nanoflake, and size of the nanoflake. Conclusions are discussed in Section4.

Received: November 4, 2013
Published: January 14, 2014

2. COMPUTATIONAL METHODS

The molecular dynamics simulations in this work are based on the open source code LAMMPS developed by Sandia National Laboratories.[33] Langevin dynamics and periodic boundary conditions are employed to set up the simulation system. To best capture the behavior of the carbon surfaces we utilize the adaptive intermolecular reactive empirical bond order (AIREBO) potential for intragraphene carbons as described by Stuart et al.[34] as

$$E = \frac{1}{2}\sum_{i}\sum_{j\neq i}\left[E_{ij}^{REBO} + E_{ij}^{LJ} + \sum_{k\neq i,j}\sum_{l\neq i,j,k} E_{kijl}^{TORSION}\right] \quad (1)$$

where the E^{REBO} term is the REBO potential,[35] shown as

$$E_{ij}^{REBO} = V_{ij}^{R}(r_{ij}) + b_{ij}V_{ij}^{A}(r_{ij}) \quad (2)$$

where V_{ij}^{R} is a repulsive term, V_{ij}^{A} is an attractive term, and b_{ij} is the environmental-dependent bond order term between atoms, which activates the attractive term only for bonded atoms. The AIREBO potential is best suited for systems of hydrogen and carbon, rendering the all-carbon system well-defined. Because the REBO potential only accounts for interactions of atoms within two Angstroms of one another, the AIREBO potential also includes the E^{LJ} term, which is a standard 12-6 Lennard Jones potential for distances 2 Å < r < cutoff. The cutoff for the LJ term is set here to be 10.2 Å as a good balance between computation speed and accuracy. The AIREBO potential also includes the $E^{TORSION}$ term, which is a four-body potential describing hydrocarbon dihedral angle preference. The potential between discrete sheets of graphene is modeled only by a Lennard-Jones 12-6 potential, described by the equation

$$E_{ij}^{LJ} = 4\epsilon\left(\left(\frac{\sigma}{r_{ij}}\right)^{12} - \left(\frac{\sigma}{r_{ij}}\right)^{6}\right) \quad (3)$$

using a σ of 3.36 Å and an ϵ value of 2.168 meV as demonstrated for intergraphene sliding by Shibuta et al.[36]

The substrate we simulate is a single sheet of graphene 50 nm along the x direction and 10 nm along the y direction with

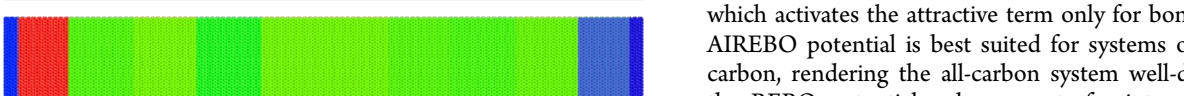

Figure 1. Computational geometry and setup of the graphene sheet. Both end stripes are the fixed atoms with blue color, the red area is the NVT controlled hot end, the light blue area is the NVT controlled cold end, and the yellow atoms in the center are not thermostatted.

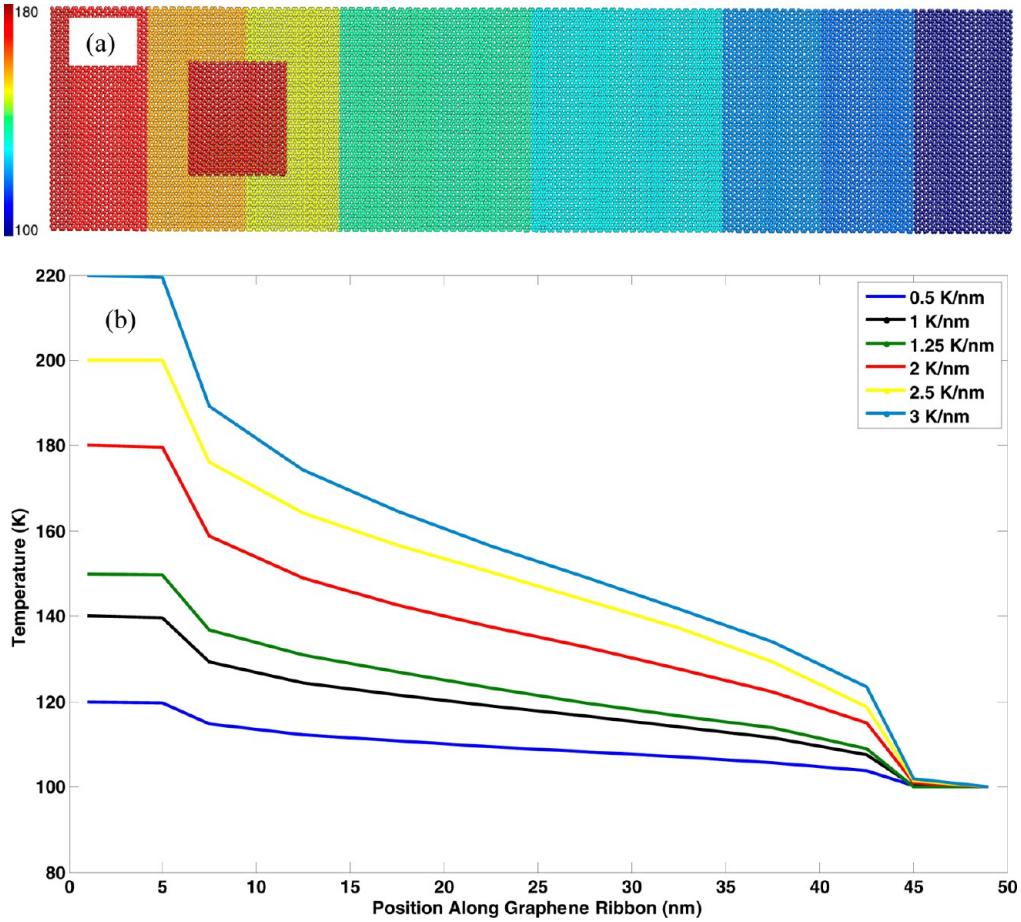

Figure 2. (a) Representation of the described setup for a temperature gradient of 80 K (2 K nm^{-1}), color coded to show the temperature profile. The first and last strips are the NVT controlled sections, whereas the center of the graphene sheet and the graphene nanoflake are not thermostatted. (b) The steady-state temperature profile for six different temperature gradients.

dx.doi.org/10.1021/ct400963d | J. Chem. Theory Comput. 2014, 10, 722−730

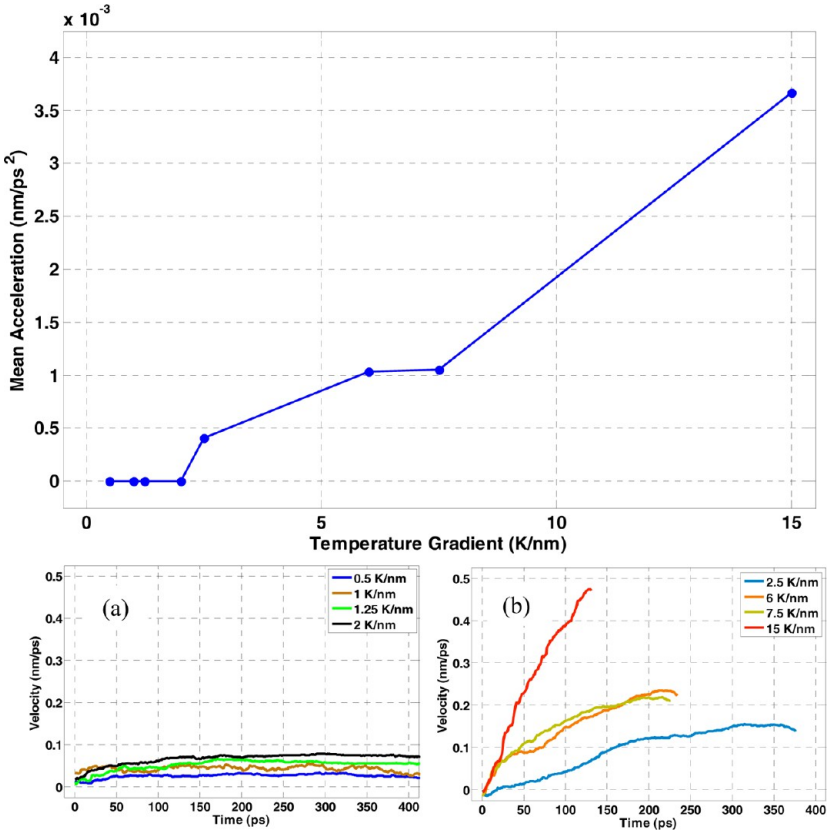

Figure 3. Averaged acceleration profile of a square nanoflake as a function of the temperature gradient. Subset a represents the velocity over time of the four zero-acceleration data points, whereas subset b represents the velocity over time of the four accelerating data points. The same axes are used for both insets for the sake of comparison.

the periodic boundary in the *y* direction concurrent with the edges of the large sheet to simulate an infinitely wide sheet. Figure 1 shows the computational setup of the graphene we simulate. The first nanometer of each of the free ends of the sheet is fixed and a thermal gradient is applied across the *x* direction. The 4 nm closest to the fixed region (shown in Figure 1) are temperature controlled using canonical NVT Nosé–Hoover thermostat with a high and low temperature, respectively. The rest of the atoms in the graphene sheet are controlled using Newtonian dynamics, with no thermostats applied. To better capture the temperature profile in graphene sheet, the region of graphene sheet not controlled by a thermostat is partitioned into eight regions with the width of 5 nm each as depicted in Figure 2a, in which the high temperature and low temperature for temperature-controlled regions are 180 and 100 K, respectively, and the linear temperature distribution in the graphene sheet as depicted in Figure 2b reproduces the Fourier's law's characteristics. A nanoflake made of graphene is placed above the large sheet at a distance of 7.5 nm from the fixed end with the higher temperature, with the entire nanoflake controlled by non-thermostat Newtonian dynamics. The entire system is allowed to run for 2 ns to be certain that the thermal gradient across the graphene sheet is stable for the further investigations. During this initial phase, the center of mass of the nanoflake is constrained to prevent motion. At the end of the initial phase, the constraint is released and the nanoflake is allowed to move freely. After temperature equilibrium status, the system is allowed to run for 1 ns and the result is documented for further analysis. To better present the effect of temperature gradient on the motion of a nanoflake, the temperature of the cold end of the system is fixed as 100 K for each run while the temperature of the hot end is set as a variety of values to provide the desired thermal gradient. Also, to investigate the effect of the geometry of a nanoflake on its motion, various geometries such as circular, square, rectangular shapes are constructed to perform the simulations for better understanding the impact of shape on thermophoretic motion while the area of the graphene nanoflake is kept constant at 25 nm^2 no matter which shape it is.

3. RESULTS AND DISCUSSION

Effects of Temperature Gradient on Nanoflake Motion. From the energetic perspective, moving a nanostructure on the graphene surface requires a sufficient driving force to overcome the intrinsic friction barrier due to the adhesion interactions. The temperature gradient in graphene provides a feasible way for generating sufficient energy due to thermophoresis to surpass the barrier, as indicated by previous works.[37,38] However, the relationship between the velocity or acceleration of motion bestowed by graphene and its temperature gradient remains to be further explored. In what follows, we apply to the simulation system described in Figure 1 eight different temperature gradients with values of 0.5, 1, 1.25, 2, 2.5, 6, 7.5, and 15 K nm^{-1}.

Figure 3 depicts the correlation of the temperature gradient and the motion of a nanoflake with square shape and area of 25 nm^2. The graphene sample travels from the hotter end to the colder end at a nearly constant acceleration dependent on the temperature gradient, as indicated in Figure 3. Figure 4

dx.doi.org/10.1021/ct400963d | J. Chem. Theory Comput. 2014, 10, 722–730

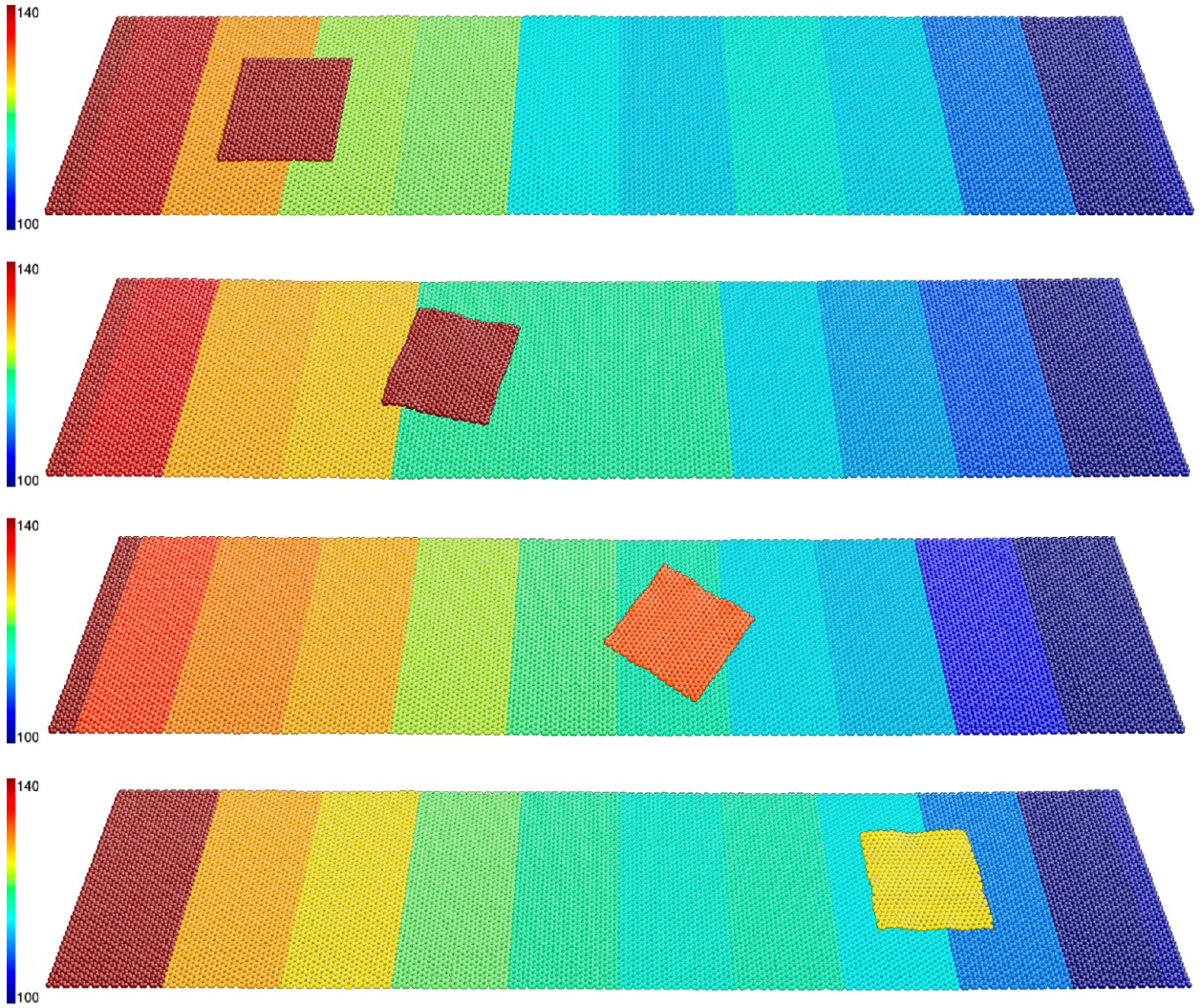

Figure 4. Dynamic motion of a square nanoflake on the graphene sheet with temperature gradient of 1 K nm^{-1}. Images shown are 0, 170, 345, and 585 ps after the center of mass of the nanoflake is unrestrained.

demonstrates the evolution of a nanoflake with a square shape across the graphene sheet at a temperature gradient of 1 K nm^{-1}. The nanoflake moves with a nearly constant velocity of 0.04 nm ps^{-1}, as evidenced by Figure 3, accompanying a rotational motion with angular velocity of 4.4 revolutions ns^{-1}. At temperature gradients of 0.5, 1, 1.5, and 2 K nm^{-1}, the acceleration of the nanoflake is close to 0, and the final velocity when it reaches to the cold end is 33.4, 39.2, 45.3, and 58.6 nm ns^{-1}, respectively; while at temperature gradients of 2.5, 6, 7.5, and 15 K nm^{-1}, the acceleration of the nanoflake is 0.49, 1.01, 1.09, and 3.65 pm ps^{-2}, respectively. As expected, the high temperature gradient creates a large initial driving force to move the nanoflake indicated in its acceleration profile. The acceleration in the nanoflake demonstrates that the temperature gradient provides a net initial driving force on the nanoflake due to an imbalance between phonon wave packets moving from the higher temperature region to lower temperature region of the nanoflake. At lower temperature gradients, the nanoflake experiences a constant velocity once the systems reaches a steady status whereas at higher temperature gradients, the nanoflakes travels with a constant acceleration, which indicates that there exists a threshold temperature gradient across the graphene which distinguishes the motion capability of nanoflakes. In the case of a nanoflake with an area of 25 nm^2, the threshold temperature gradient is 2 K nm^{-1} based on multiple repeated cases with the same initial condition. In a set of trials run with a square nanoflake of area 36 nm^2 a similar threshold temperature gradient is evidenced, indicating that at least for similarly sized nanoflakes there is a distinct gradient threshold below which the nanoflake does not accelerate but instead achieves a constant velocity. Thereby, this finding unveils a novel way to control the motion of nanoparticles or nanostructures on the surface of graphene and further provides an intriguing way to manipulate the particles at nanoscale. The zero acceleration for low temperature gradients indicates a balance of forces, and implies that the thermophoretic driving force is being countered by some other forces such as friction, and therefore further exploration into the nature and effect of the various forces at play is performed in the following sections.

Effects of Temperature Gradient of Graphene on Driving Forces of Nanoflake. How to precisely transport or manipulate the particle to a targeted area at a targeted time at the nanoscale heavily depends on the fundamental understanding of the driving force emanated from a variety of sources, such as temperature gradient in this study. To determine the correlation of mean driving force acting on the

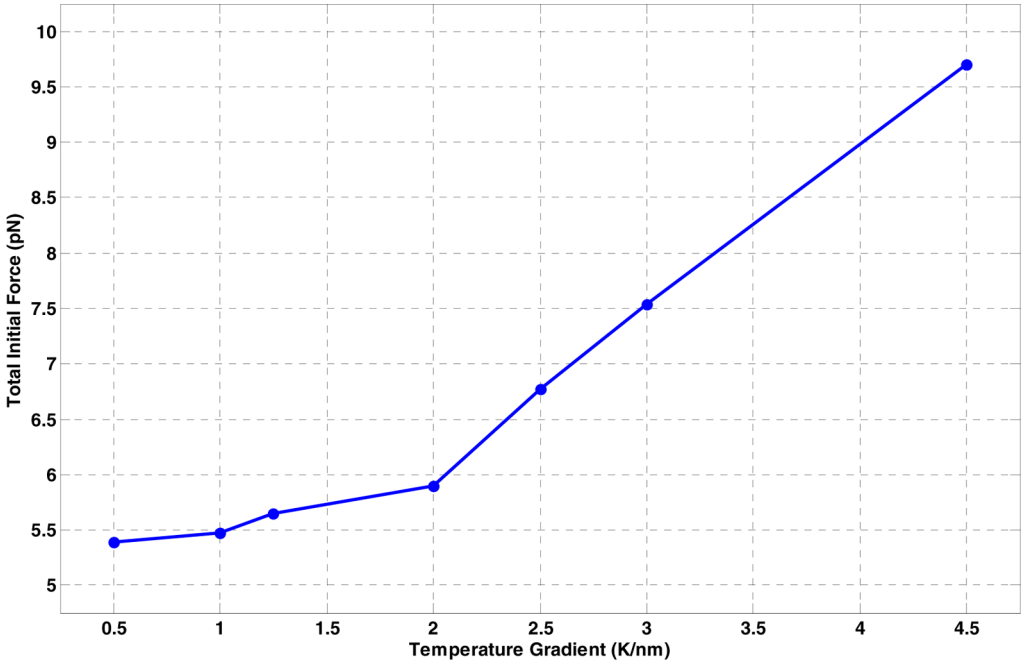

Figure 5. Total initial driving force versus temperature gradient of the system with square shaped nanoflake.

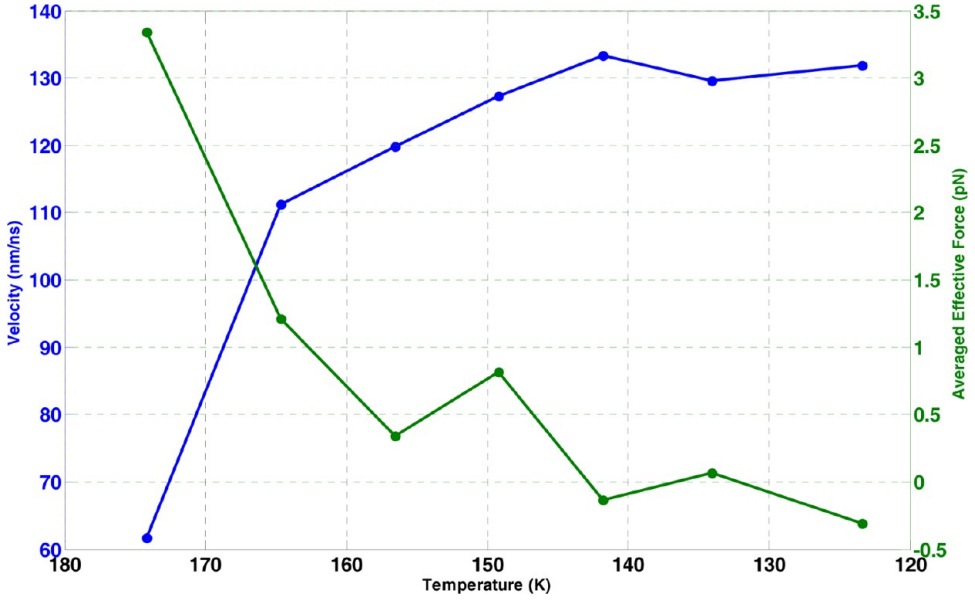

Figure 6. Real-time velocity and effective driving force of squared nanoflake across the temperature profile at a temperature gradient of 2 K nm^{-1}.

graphene nanoflake with the applied temperature gradient, a steered molecular dynamics setup is applied.[39,40] This setup consists of a spring with one end fixed and the other attached to the nanoflake aligned parallel to the x-axis. As the temperature gradient is increased, the nanoflake moves away from its initial position at the high end of the temperature gradient and the force applied is calculated by the average position difference multiplied by the spring constant. For each temperature gradient, the system is allowed to come to a steady state and then the average change from the equilibrium position over 1 ns is calculated. The effective driving force is derived from the spring constant k and difference from equilibrium position x by using the equation $F_{eff} = k\bar{x}$, where k is 1 meV nm^{-1}. In addition to the thermophoretic driving force, this summation of forces must include a counteractive frictional force to account for the constant-velocity movement of the nanoflake at low temperature gradients after it reaches the steady status. In this case, the equation can be written as

$$F_T - F_f + \xi(t) = k\bar{x} \quad (4)$$

where $\xi(t)$ is the thermal noise generated by the system. The thermal noise is treated as an average of zero, with any bias instead contributing to the thermophoretic force. To determine the effect of friction on the system, a second set of steered molecular dynamics simulations are performed in which there is no temperature gradient; both ends of the sheet are kept at 100 K. The nanoflake is connected by a spring to an artificial particle moving at a constant velocity parallel to the x-axis of the system. Only the center of mass of the nanoflake is constrained; i.e., the nanoflake is free to rotate while traveling.

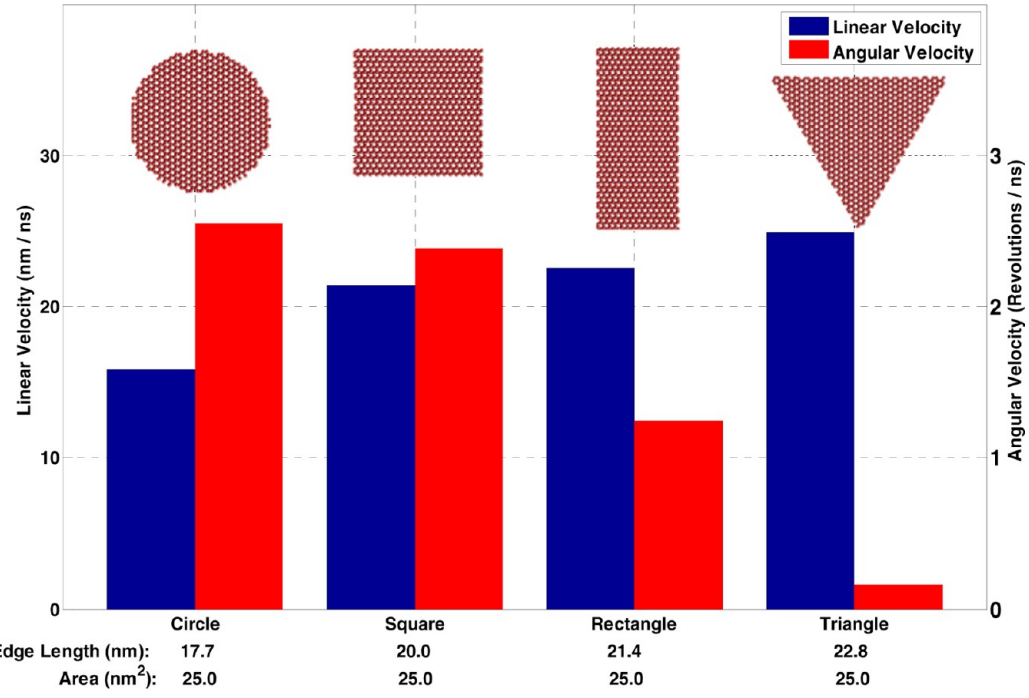

Figure 7. Linear velocity and angular velocity of nanoflakes with different geometrical shapes at a temperature gradient of 0.5 K nm^{-1}.

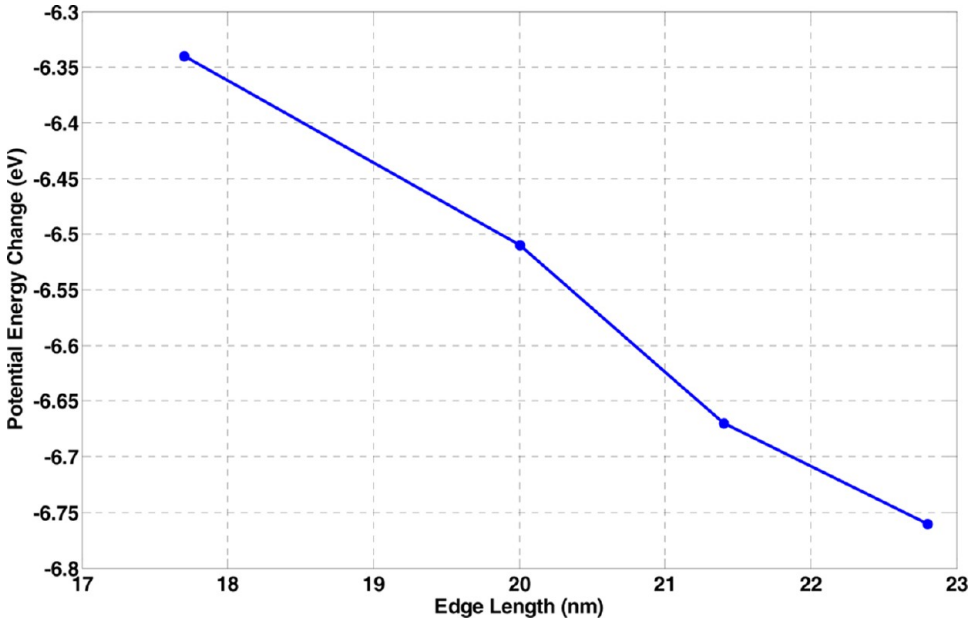

Figure 8. Potential energy change of nanoflakes with different shapes across a temperature gradient of 1 K nm^{-1} versus edge length of each nanoflake shown in Figure 7.

The amount of stretch in the spring along with the force constant is used to determine the effective frictional force of the system. The average frictional force caused by the interaction between the nanoflake and the graphene sheet at 100 K is determined to be 2.15 pN, which shows a great agreement with the value previously demonstrated superlubricity of graphene sliding.[41] The total initial thermophoretic force, as determined by the addition of the frictional force to the effective initial driving force, is listed by temperature gradients in Figure 5. At temperature gradients of 0.5, 1, 1.25, and 2 K nm^{-1}, the initial effective driving force is 3.24, 3.32, 3.49, and 3.74 pN, respectively, but above 2 K nm^{-1}, the driving force experiences a pronounced increase with consistency of the acceleration profiles depicted in Figure 3. At temperature gradients of 2.5, 3, and 4.5 K nm^{-1} the measured initial driving forces are 4.6, 5.39, and 7.55 pN. This force analysis clearly shows the evidence for the constant velocity at low temperature gradients, and the constant acceleration of high temperature gradients after these cases reaches the steady status. It is interesting to note that the effective real-time driving force decreases and the real-time velocity increases across the entire of graphene sheet with a specified temperature gradient, as indicated in Figure 6. The effective transient driving force decreases due to a combination of lower potential energy as the temperature decreases and

dx.doi.org/10.1021/ct400963d | J. Chem. Theory Comput. 2014, 10, 722−730

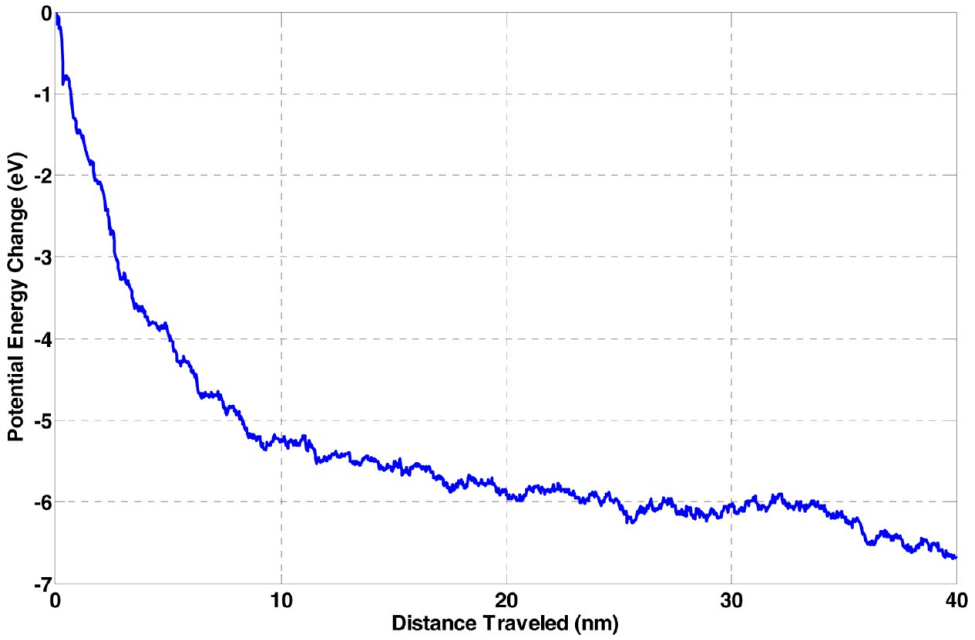

Figure 9. Evolution of potential energy change of triangular nanoflake as it travels along the graphene sheet with a temperature gradient of 0.5 K nm^{-1}.

frictional resistance. Therefore, the steady state driving force when the system reaches to steady state can be close to zero resulting in the zero acceleration motion below the threshold temperature gradient. This behavior is most notable at the threshold temperature gradient of 2 K nm^{-1}, because at lower temperature gradients, the friction force dominates whereas at higher gradients, the thermophoretic driving force dominates. The initial driving force of the nanoflake is mostly attributed to the temperature gradient, but to get an in-depth view of the behavior of the thermophoretic effect, edge effects on the nanoflake need to be further explored.

Effect of Nanoflake Geometry on Its Motion. When transporting nanoscale materials on a solid surface, a large variety of geometries and sizes has been encountered in a wealth of applications such as material synthesis. Analogous to the surface effect of 3D materials, edge effect of 2D materials has emerged as a significant factor in altering the properties of nanostructures.[42,43] Although there has been some work dealing with size variation in carbon material thermophoresis,[32] the effect of geometry has remained unexplored. To better understand the impact that the geometry of the nanoflake has on its thermophoretic motion, four different shapes are constructed and then placed upon the large graphene sheet with the specified temperature gradient as described above. To eliminate the effects from other factors such as the size of area and the reference temperature, we make all setups identical except the geometry of the nanoflakes. Each nanoflake chosen is composed of 1008 carbon atoms, which in the hexagonal graphene configuration occupies approximately 25 nm^2. The nanoflakes simulated are a square, a rectangular sheet with one edge twice that of the other, a circle, and an equilateral triangle. We have to admit that during the simulation, it is impossible to cover all possible initial conditions for a precise statistical conclusion. So, for each shape, five repeating simulations have been performed to improve the accuracy of results. The average motions of each nanoflake with specific geometry are diagrammed in Figure 7. The square and circular nanoflakes demonstrate a greater propensity to freely revolve during the motion process than the ones with triangular and rectangular geometries, possibly due to the increased orientation-dependent edge effects caused by the temperature gradient. The shapes with the largest edge perimeter are preferentially less inclined to rotate while also possessing the greatest averaged linear velocity. This may be caused by the edge effects in the geometries with longer boundaries, such as the rectangle or triangle. The square and circle have more rotationally symmetrical edges, and thus perturbative thermal effects can more easily induce an angular velocity. The number of edge carbons exhibits a direct correlation with the amount of change in potential energy of the nanoflake across the thermal gradient, as demonstrated in Figure 8, which illustrates that the magnitude of the change in potential energy increases monotonically as the edge length increases for the tested geometries with the same surface area. As the number of carbons in the nanoflake is kept constant, the edge geometry of the nanoflake is the prime factor contributing to this difference. A nanoflake with a larger number of edge carbons accompanies with a larger drop in potential energy as the nanoflake evolves to a more energetically favorable position, i.e., the cold end of the temperature gradient. For the circular, square, rectangular, and triangular nanoflakes, the potential energy difference across a temperature gradient of 1 K nm^{-1} is 6.34, 6.51, 6.67, and 6.76 eV, respectively, which provides potential quantitative evidence to support the correlation between the linear velocity and the edge effect of nanoflake described in Figure 7. Figure 9 shows a close-up of the evolution of the potential energy with respect to the displacement the triangle nanoflake travels and the other geometries exhibit similar potential energy drops, which depicts that the potential energy of the nanoflake decreases as it travels toward the end of graphene sheet with low temperature. The nanoflake clearly moves toward the most energetically favorable position in which the nanoflake possesses lower potential energy. These findings offer the novel insights into controlling the motions, rotation and translation, of the nanosystem by manipulating its geometric shape.

4. CONCLUSIONS

In summary, we have utilized nonequilibrium molecular dynamics simulations to investigate the effects of various factors such as substrate temperature gradient and nanoflake edge geometry on the thermophoretic motion of a graphene nanoflake across a 50 nm long graphene substrate. The thermophoretic driving force is posited to be a discrepancy across the temperature gradient in the kinetic energy imparted to the nanoflake due to the interaction with the graphene sheet; i.e., the part of the nanoflake that interacts with a higher temperature portion of the graphene sheet receives more kinetic energy than the part interactive with a lower temperature portion, resulting in a force imbalance across the nanoflake. We have successfully quantitatively calibrated the frictional force and effective driving force across a range of temperature gradients. Our findings show that a larger temperature gradient generates faster motion of the nanoflake in the direction opposite to the gradient, which provides a novel concept to manipulate the motion of the particle at nanoscale. There is a key thermal gradient between 2 and 2.5 K nm^{-1} for nanoflakes 25 nm^2 in area where the thermophoretic driving force undergoes a large increase in magnitude, leading to a constant acceleration of particles as they overcome the relatively weak friction force of intergraphene sliding. Our simulations also demonstrate that the geometry and edge effects of the nanoflake can have a noticeable effect on the translational and rotational motion of the nanoflake. The inverse correlation between edge length and average angular velocity is quite intriguing, which indicates that the edge of the nanoflake is quite important to its thermophoretic motion. This work provides a comprehensive approach to intergraphene thermophoretic motion necessary to develop novel methods of nanotransportation and the fine positioning of nanoparticles.

AUTHOR INFORMATION

Corresponding Author

*Xianqiao Wang. E-mail: xqwang@uga.edu.

Notes

The authors declare no competing financial interest.

ACKNOWLEDGMENTS

The authors acknowledge support from the University of Georgia (UGA) Research Foundation. Calculations are performed at the UGA Advanced Computing Resource Centre.

REFERENCES

(1) Le Rouzic, J.; Vairac, P.; Cavallier, B.; Cretin, B. W-Shaped Cantilevers for Scanning Force Microscopy. *IEEE Sens. J.* **2013**, *13* (4), 1340−1346.

(2) Ziegler, D.; Meyer, T. R.; Farnham, R.; Brune, C.; Bertozzi, A. L.; Ashby, P. D. Improved accuracy and speed in scanning probe microscopy by image reconstruction from non-gridded position sensor data. *Nanotechnology* **2013**, *24* (33), 335703.

(3) Wang, C. M.; Itoh, H. A simulation study for evaluating and improving the accuracy of surface roughness measured by atomic force microscopy. *Meas. Sci. Technol.* **2013**, *24* (3), 035401.

(4) Mullenbroich, M. C.; McAlinden, N.; Wright, A. J. Adaptive optics in an optical trapping system for enhanced lateral trap stiffness at depth. *J. Opt. (Bristol, U. K.)* **2013**, *15* (7), 075305.

(5) Michihata, M.; Yoshikane, T.; Hayashi, T.; Takaya, Y. New Technique for Single-Beam Gradient-Force Laser Trapping in Air. *Int. J. Optomechatron.* **2013**, *7* (1), 46−59.

(6) Lansdorp, B. M.; Tabrizi, S. J.; Dittmore, A.; Saleh, O. A. A high-speed magnetic tweezer beyond 10,000 frames per second. *Rev. Sci. Instrum.* **2013**, *84* (4), 044301.

(7) Bryant, Z.; Oberstrass, F. C.; Basu, A. Recent developments in single-molecule DNA mechanics. *Curr. Opin. Struct. Biol.* **2012**, *22* (3), 304−312.

(8) Guillonneau, G.; Kermouche, G.; Bec, S.; Loubet, J. L. Determination of mechanical properties by nanoindentation independently of indentation depth measurement. *J. Mater. Res.* **2012**, *27* (19), 2551−2560.

(9) Moy, C. K. S.; Bocciarelli, M.; Ringer, S. P.; Ranzi, G. Indentation and imprint mapping for the identification of material properties in multi-layered systems. *Comput. Mater. Sci.* **2011**, *50* (5), 1681−1691.

(10) Omidi, E.; Korayem, A. H.; Korayem, M. H. Sensitivity analysis of nanoparticles pushing manipulation by AFM in a robust controlled process. *Precis. Eng.* **2013**, *37* (3), 658−670.

(11) Reyes, D. R.; Mijares, G. I.; Nablo, B.; Briggman, K. A.; Gaitan, M. Trapping and release of citrate-capped gold nanoparticles. *Appl. Surf. Sci.* **2011**, *257* (20), 8373−8377.

(12) Whitehill, J. D.; Gralinski, I.; Joiner, D.; Neild, A. Nanoparticle manipulation within a microscale acoustofluidic droplet. *J. Nanopart. Res.* **2012**, *14* (11), 1−11.

(13) Xu, L. J.; Han, G. B.; Hu, J. W.; He, Y.; Pan, J. G.; Li, Y. J.; Xiang, J. N. Hydrophobic coating- and surface active solvent-mediated self-assembly of charged gold and silver nanoparticles at water-air and water-oil interfaces. *Phys. Chem. Chem. Phys.* **2009**, *11* (30), 6490−6497.

(14) Azong-Wara, N.; Asbach, C.; Stahlmecke, B.; Fissan, H.; Kaminski, H.; Plitzko, S.; Bathen, D.; Kuhlbusch, T. A. J. Design and experimental evaluation of a new nanoparticle thermophoretic personal sampler. *J. Nanopart. Res.* **2013**, *15* (4), 1−12.

(15) Barreiro, A.; Rurali, R.; Hernandez, E. R.; Moser, J.; Pichler, T.; Forro, L.; Bachtold, A. Subnanometer motion of cargoes driven by thermal gradients along carbon nanotubes. *Science* **2008**, *320* (5877), 775−778.

(16) Piazza, R. Thermophoresis: moving particles with thermal gradients. *Soft Matter* **2008**, *4* (9), 1740−1744.

(17) Shenai, P. M.; Xu, Z. P.; Zhao, Y. Thermal-gradient-induced interaction energy ramp and actuation of relative axial motion in short-sleeved double-walled carbon nanotubes. *Nanotechnology* **2011**, *22* (48), 485702.

(18) Guo, Z. R.; Chang, T. C.; Guo, X. M.; Gao, H. J. Mechanics of thermophoretic and thermally induced edge forces in carbon nanotube nanodevices. *J. Mech. Phys. Solids* **2012**, *60* (9), 1676−1687.

(19) Shenai, P. M.; Ye, J.; Zhao, Y. Sustained smooth dynamics in short-sleeved nanobearings based on double-walled carbon nanotubes. *Nanotechnology* **2010**, *21* (49), 495303.

(20) Feng, X. F.; Kwon, S.; Park, J. Y.; Salmeron, M. Superlubric Sliding of Graphene Nanoflakes on Graphene. *ACS Nano* **2013**, *7* (2), 1718−1724.

(21) Zhang, X. H.; Santoro, G. E.; Tartaglino, U.; Tosatti, E. Dynamical phenomena in fast sliding nanotube models. *Philos. Mag.* **2013**, *93* (8), 922−948.

(22) Bourlon, B.; Glattli, D. C.; Miko, C.; Forro, L.; Bachtold, A. Carbon nanotube based bearing for rotational motions. *Nano Lett.* **2004**, *4* (4), 709−712.

(23) Tangney, P.; Louie, S. G.; Cohen, M. L. Dynamic sliding friction between concentric carbon nanotubes. *Phys. Rev. Lett.* **2004**, *93* (6), 065503.

(24) Tu, Z. C.; Ou-Yang, Z. C. A molecular motor constructed from a double-walled carbon nanotube driven by temperature variation. *J. Phys.: Condens. Matter* **2004**, *16* (8), 1287−1292.

(25) Schoen, P. A. E.; Walther, J. H.; Arcidiacono, S.; Poulikakos, D.; Koumoutsakos, P. Nanoparticle traffic on helical tracks: Thermophoretic mass transport through carbon nanotubes. *Nano Lett.* **2006**, *6* (9), 1910−1917.

(26) Schoen, P. A. E.; Walther, J. H.; Poulikakos, D.; Koumoutsakos, P. Phonon assisted thermophoretic motion of gold nanoparticles

inside carbon nanotubes. *Appl. Phys. Lett.* **2007**, *90* (25), 253116−253116.
(27) Hou, Q. W.; Cao, B. Y.; Guo, Z. Y. Thermal gradient induced actuation in double-walled carbon nanotubes. *Nanotechnology* **2009**, *20* (49), 495−503.
(28) Rurali, R.; Hernandez, E. R. Thermally induced directed motion of fullerene clusters encapsulated in carbon nanotubes. *Chem. Phys. Lett.* **2010**, *497* (1−3), 62−65.
(29) Wei, N.; Wang, H. Q.; Zheng, J. C. Nanoparticle manipulation by thermal gradient. *Nanoscale Res. Lett.* **2012**, *7*, 1−9.
(30) Santamaria-Holek, I.; Reguera, D.; Rubi, J. M. Carbon-Nanotube-Based Motor Driven by a Thermal Gradient. *J. Phys. Chem. C* **2013**, *117* (6), 3109−3113.
(31) Guo, Y. F.; Guo, W. L. Soliton-like thermophoresis of graphene wrinkles. *Nanoscale* **2013**, *5* (1), 318−323.
(32) Savin, A. V.; Kivshar, Y. S. Transport of fullerene molecules along graphene nanoribbons. *Sci. Rep. (U. K.)* **2012**, *2*, 1−12.
(33) Plimpton, S. Fast Parallel Algorithms for Short-Range Molecular-Dynamics. *J Comput. Phys.* **1995**, *117* (1), 1−19.
(34) Stuart, S. J.; Tutein, A. B.; Harrison, J. A. A reactive potential for hydrocarbons with intermolecular interactions. *J. Chem. Phys.* **2000**, *112* (14), 6472−6486.
(35) Brenner, D. W.; Shenderova, O. A.; Harrison, J. A.; Stuart, S. J.; Ni, B.; Sinnott, S. B. A second-generation reactive empirical bond order (REBO) potential energy expression for hydrocarbons. *J. Phys.: Condens. Matter* **2002**, *14* (4), 783−802.
(36) Shibuta, Y.; Elliott, J. A. Interaction between two graphene sheets with a turbostratic orientational relationship. *Chem. Phys. Lett.* **2011**, *512* (4−6), 146−150.
(37) Lohrasebi, A.; Neek-Amal, M.; Ejtehadi, M. R. Directed motion of C-60 on a graphene sheet subjected to a temperature gradient. *Phys. Rev. E* **2011**, *83* (4), 042601−4.
(38) Zambrano, H. A.; Walther, J. H.; Jaffe, R. L. Thermally driven molecular linear motors: A molecular dynamics study. *J. Chem. Phys.* **2009**, *131* (24), 241104.
(39) Lei, Y.; Leng, Y. Hydrophobic drying and hysteresis at different length scales by molecular dynamics simulations. *Langmuir* **2012**, *28* (6), 3152−3158.
(40) Wang, H.; Leng, Y. Molecular dynamics simulations of the stable structures of single atomic contacts in gold nanojunctions. *Phys. Rev. B* **2011**, *84* (24), 245422.
(41) Verhoeven, G.; Dienwiebel, M.; Frenken, J. Model calculations of superlubricity of graphite. *Phys. Rev. B* **2004**, *70* (16), 165418.
(42) Kitamura, T.; Hirakata, H.; Itsuji, T. Effect of residual stress on delamination from interface edge between nano-films. *Eng. Fract. Mech.* **2003**, *70* (15), 2089−2101.
(43) Lin, Z. C.; Chou, M. H. A Simulative Measuring Model of Scanning Near-Field Optical Microscope by Applying Aluminum Atoms of FCC Structure for The Nano-Scale Standard Sample and The Qualitative Analysis. *J. Chin. Soc. Mech. Eng.* **2009**, *30* (1), 1−6.